

Analyses of the Dynamic Properties of Nuclear Lamins by Fluorescence Recovery After Photobleaching (FRAP) and Fluorescence Correlation Spectroscopy (FCS)

Shimi Takeshi, Chan-Gi Pack, and Robert D. Goldman

Abstract

The major structural components of the nuclear lamina are the A- and B-type nuclear lamin proteins which are also present in the nucleoplasm. Studies of molecular movements of the lamins in both the lamina and nucleoplasm of living cell nuclei have provided insights into their roles in maintaining nuclear architecture. In this chapter, we present protocols for quantitatively measuring the mobilities of lamin proteins by fluorescence recovery after photobleaching (FRAP) and fluorescence correlation spectroscopy (FCS) in mammalian cell nuclei.

Key words Lamina, Lamin, FRAP, FCS

1 Introduction

In mammalian cells, the nuclear lamina (NL) lies between the inner membrane of the nuclear envelope (NE) and chromatin. There are four nuclear lamin isoforms which collectively are the major structural proteins in the NL [1]. The four isoforms include lamins A (LA), C (LC), B1 (LB1), and B2 (LB2). These proteins play important roles in regulating the size, shape, and stiffness of the nucleus, and they are thought to be involved in chromatin organization, transcription, DNA replication, and DNA repair [2]. The lamins contain an α -helical central rod domain with mainly non- α -helical N- and C-terminal domains [3]. These isoforms polymerize into filamentous structures as determined by electron microscopy [4] and more recently by three-dimensional structured illumination microscopy (3D-SIM) [5]. Confocal microscopic observations have shown that A- and B-type lamin fibrils appear to form separate but interacting meshworks [6]. A minor fraction of lamins is also present in the nucleoplasm [6, 7]. The mechanisms for regulating the assembly and disassembly of the NL involve

phosphorylation and dephosphorylation during both interphase and mitosis. In interphase nuclei, there is a fraction of LA/C in the nucleoplasm which is phosphorylated, apparently preventing the incorporation of these two isoforms from being incorporated into the filamentous structures comprising the NL [8].

Live cell imaging with fluorescently labeled lamins has provided important insights into their dynamic properties. Live cell imaging techniques that have been used for analyzing lamin dynamics include fluorescence recovery after photobleaching (FRAP) and fluorescence correlation spectroscopy (FCS). These two techniques have been used to quantitatively determine the mobilities of fluorescently labeled lamins within the nuclei of living cells. FRAP studies have revealed that the lamin subunit mobilities and exchange rates are much slower in the NL, while FCS has revealed that some lamin isoforms exhibit high mobilities within the nucleoplasm. Using GFP-tagged wild-type and mutant lamin isoforms, studies by FRAP and FCS have revealed the kinetics of their association and disassociation from the NL and their diffusion coefficients in the nucleoplasm. For example, we and others have shown by FRAP that <25 % of GFP-LA and LC in the NL are exchanged within 10 min [7–11], indicating that LA/C is immobile in the NL. On the other hand, LA/C in the nucleoplasm is highly mobile as their diffusion coefficients determined by FCS are between ~ 0.4 and $\sim 5.6 \mu\text{m}^2/\text{s}$ [6].

2 Materials

2.1 *Microscope and Sample Setup for FRAP*

1. Live cell imaging chamber: Glass bottom microwell dishes (35 mm petri dish, 20 mm microwell, No. 1.5 cover glass, No. P35G-1.5-20-C, Mat-Tek).
2. Culture medium for microscopy: Leibovitz's L15 medium (phenol-red free, Life Technologies) containing 10 % serum and antibiotics (i.e., penicillin and streptomycin).
3. HeLa cells transfected with GFP-LA cultured for 48–72 h after transfection [6].
4. Spinning disk confocal microscope. A setup such as a Nikon Ti Perfect Focus microscope (Nikon) with CF160 lenses and equipped with a Yokogawa CSU-X1 spinning disk unit (Yokogawa) and an iXon 3 14-bit EM CCD camera (Andor Technology) is ideal for FRAP studies.
5. Laser for photobleaching GFP-LA fluorescence: 488 nm argon laser line.
6. Temperature and CO₂ control must be maintained. For this purpose, we use a Tokai-HIT stage-top incubator set for 37 °C and 5 % CO₂.

2.2 Data Analysis for FRAP

Andor iQ2 (Andor Technology) and Prism 6 (GraphPad) software

2.3 Microscope and Sample Setup for FCS

1. Live cell imaging chamber: 8-well with No. 1.0 or No. 1.5 borosilicate chambered cover glass (Lab-Tek or Lab-Tek II, Nunc).
2. Culture medium for microscopy: Opti-MEM I reduced serum medium (phenol-red free, Life Technologies).
3. HeLa cells transfected with GFP-LA and cultured for 48–72 h after transfection.
4. Zeiss LSM 510 Microscope equipped with a water-immersion objective lens (C-Apochromat 40 \times , 1.2 NA) and a Zeiss ConfoCor 2 spectrometer.
5. Laser for FCS: 488-nm argon laser line
6. Calibration for FCS: rhodamine 6G [Rh6G] fluorescent dye – 10⁻⁷ M in distilled water solution.

2.4 Data Analysis for FCS

LSM510 ConfoCor 2 (Carl Zeiss) software

3 Methods**3.1 Cell Culture and Transfection**

1. Grow HeLa cells on a 10 cm cell culture plastic dish under a humidified 5 % CO₂ atmosphere at 37 °C in Dulbecco's modified Eagle's medium (DMEM) supplemented with 10 % fetal calf serum and antibiotics (penicillin and streptomycin).
2. Detach when cells are 80–90 % confluent using 0.05 % trypsin-EDTA solution and then centrifuge at 200 $\times g$ for 5 min followed by resuspension in 500 μ L of DMEM.
3. Transfer the cell suspension into a 4 mm electroporation cuvette, and then add 10 μ g of the 5 plasmid-encoding GFP-LA.
4. Electroporate at 260 V and 950 μ F.
5. Add 5.0 mL of DMEM supplemented with 10 % FCS and antibiotics, pipette up and down, and place cells immediately into a 100 mm culture dish.
6. ~6 h after incubation in a tissue culture incubator, change the medium with fresh DMEM supplemented with 10 % FCS and antibiotics.
7. Incubate for ~24 h in a CO₂ incubator.
8. Trypsinize and replate the electroporated cells at ~15 % density (5 \times 10⁴ cells) onto a glass bottom microwell dish for FRAP or 8-well with No. 1.0 or No. 1.5 borosilicate chambered cover glass for FCS.
9. Incubate for ~24 h in a tissue culture incubator (*see Note 1*).

3.2 FRAP

1. Make sure that the objective and laser are perfectly aligned as per manufacturer's instructions.
2. Overlay cells with Leibovitz's L15 medium containing 10 % serum and antibiotics including penicillin and streptomycin.
3. Incubate cells 37 °C and under 5 % CO₂ for at least 30 min before microscopic observation.
4. Equilibrate a CO₂ incubator (see above) mounted on the microscope stage at 37 °C for 30 min.
5. Open imaging software (e.g., NIS-Elements) and setup FRAP conditions following manufacturer's protocol (laser power, dwelling time, timing of imaging pre- and post-bleaching and time-lapse setting).
6. Place a dish onto the stage.
7. Find the correct focus and switch on the stage control to maintain focus (e.g., Nikon Perfect Focus System). Maintaining focus is essential throughout FRAP measurements (Fig. 1).

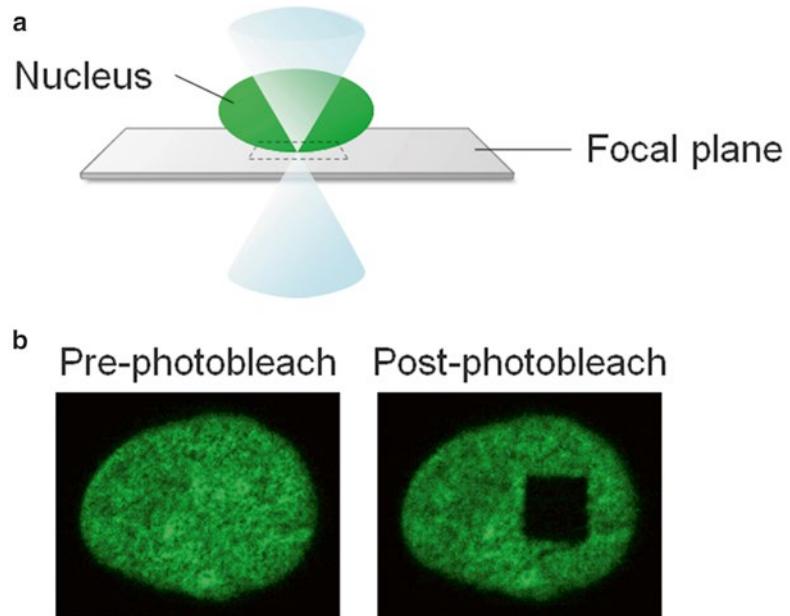


Fig. 1 Procedure of fluorescence recovery after photobleaching (FRAP) measurement on GFP-LA in the NL of living cell nuclei. **(a)** FRAP measurement is performed as shown in a schematic diagram. Fluorescence signals of GFP-LA are detected in the NL region at the bottom of the nucleus to visualize a maximally flat surface. A focus drift from the region is automatically corrected by a real-time correction system (see also text). **(b)** Representative fluorescence images of GFP-LA in living HeLa cells were taken at the lower nuclear surface by confocal microscopy immediately before and after a square region are photobleached

3.3 Performing a Test Bleach

The key to success for a FRAP experiment is the proper setting of photobleaching and acquisition conditions. It is essential that sufficient time is devoted to optimizing these conditions. First perform a test bleach to optimize bleach times, duration time, and region of interest (ROI) within the NL. Then optimize image acquisition conditions for monitoring the recovery of the fluorescent signal using time-lapse imaging with a well-equipped spinning disk confocal microscope (see above).

1. Find an area of interest using the eyepieces. Cells with moderate GFP-LA expression are recommended (*see Note 2*).
2. Make sure of the alignment of the optical axis and choose correct objective lens by following manufacturer's instruction.
3. Test photobleaching in several cells using a 488 nm laser at 100 % output to determine optimal duration time, size, and location of ROI for efficient photobleaching (*see Note 3*).
4. Roughly estimate the timescale required for the fluorescence recovery of GFP-LA in the mobile fraction.
5. Optimize image acquisition conditions including scanning speed, time intervals, and duration time for imaging and choose adequate laser wavelength and adjust the laser power at the low level to avoid any excess photobleaching by imaging. The acquisition speed should be fast enough to monitor the fluorescence recovery (*see Note 4*).

3.4 Performing a FRAP Experiment

1. Find an area of interest using the eyepieces. Cells with moderate GFP-LA expression are recommended, and if possible, other unbleached cells should be visible in the field of view (*see Note 5*).
2. Select the system to continuously acquire images of the NL (*see Note 6*). High-speed scan mode can be helpful for avoiding excess photobleaching caused by image acquisition.
3. Adjust the conditions for image acquisition (see above).
4. Choose an ROI area for photobleaching in a defined region of the NL on the acquired image. To have sufficient non-photobleached GFP-LA molecules for detecting the full fluorescence recovery in the mobile fraction, photobleached area should be <80 % of the entire lamina region.
5. Set the FRAP experiment parameters including image acquisition time, time-lapse interval, and total time period of the experiment. To measure only the fluorescence recovery of GFP-LA by the molecular exchanges but not the flow of newly synthesized GFP-LA, total time period should be at maximum 20 min.
6. Monitor cells including both non-bleached and bleached areas of the NL for the fluorescence recovery at 30 s intervals as indicated above: we use Andor iQ2 software for FRAP.

3.5 FRAP Analysis

We analyze our FRAP data using GraphPad Prism 6 software as previously described [8, 12]. The region of interest (ROI) is set on the photobleached region of the NL (ROI1), and ROI2 is selected from the background. Normalized fluorescence intensity (I) is obtained as follows:

$$100 \times \left(\frac{\text{GFP LA signals in ROI1} - \text{background signals in ROI2}}{\text{GFP LA signals in ROI1 immediately before photobleaching} - \text{background signals in ROI2}} \right)$$

As shown in Fig. 2, the mobile fraction of GFP-LA is calculated by curve-fitting the fluorescence recovery data to the following formula to estimate one-phase disassociation-association kinetics:

$$I(t) = I_0 + (I_{\text{plateau}} - I_0) (1 - \exp^{-kt}) \tag{1}$$

$I(t)$: Normalized fluorescence intensity in the bleached area at a given time t .

I_{original} : Normalized original fluorescence intensity in the photobleached area (i.e., 100 %, immediately before photobleaching).

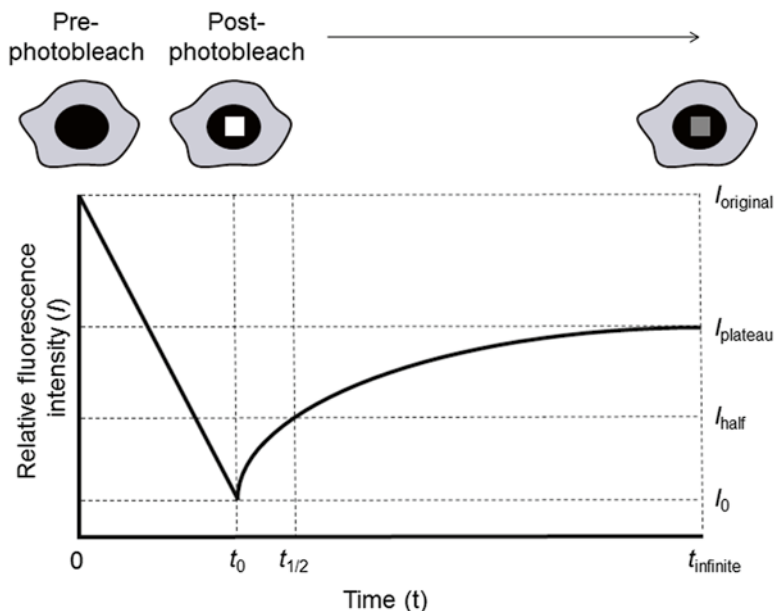


Fig. 2 An approach for curve-fitting the fluorescence recovery data is taken to estimate one-phase disassociation-association kinetics on the assumption that lamin molecules shuttle between the NL and nucleoplasm but do not laterally move along with the NL. $I(t)$, I_{original} , I_0 , I_{half} , and I_{plateau} are normalized fluorescence intensities in the bleached area at a given time t , 0 (before photobleaching), t_0 (immediately after photobleaching), $t_{1/2}$ as $\ln(2)/k$, and t_{infinite} (if experimental time continues forever), respectively. These values are computationally calculated using the equation as described in Subheading 3.5

I_0 : Normalized initial fluorescence intensity in the photo-bleached area when the t is t_0 (i.e., <20 %, immediately after photobleaching).

I_{plateau} : Normalized fluorescence intensity at plateau when the t is t_{infinite} (if experimental time continues forever).

I_{half} : $(I_{\text{plateau}} - I_0)/2$. Normalized half fluorescence intensity when the t is $t_{1/2}$.

k : Constant. It is expressed as the reciprocal of time units.

t_{half} : $t_{1/2} - t_0$. The time unit of t as $\ln(2)/k$.

3.6 ConfoCor 2 Adjustment and FCS Measurement

Solution sample containing rhodamine 6G (Rh6G) as a standard dye both for 488 and 543 nm excitation lines must be daily measured for checking correct FCS optical setup and stable confocal detection volume. Select an optical pathway on ConfoCor 2 setup for Rh6G fluorescent dye or GFP (e.g., band-pass filter, BP505-550 nm). GFP-LA will be detected with the same condition after this calibration process.

1. Place 100 μL of Rh6G solution at a concentration of 10^{-7} M in a well of an 8-well chambered cover glass.
2. Adjust the center of the objective lens at 200 μm above the upper surface of the coverslip. Adjust the correction ring of the objective lens to maximal counts per molecule (CPM in kHz) setting.
3. Adjust the pinhole size and its position by auto-adjustment according the x and y -axes. The pinhole size typically selected is equivalent to 1 Airy unit (e.g. 70 μm for 488 nm excitation in the LSM 510-ConfoCor 2 system).
4. Adjust the excitation at 488 nm to 3 %. The emission signal is detected at BP505-550 nm (green channel) for Rh6G (or GFP-LA). Excitation power for Rh6G as control can be increased up to a twofold higher value for better CPM values (i.e., high signal to noise ratio) and autocorrelation function (*see Note 7*).
5. For FCS measurements, use ten sequential repetitions of single 20 s measurement. Hardware and software packages for the ConfoCor 2 provide ten fluorescence autocorrelation functions for the ten repetitions and additionally calculate and provide an averaged autocorrelation function.
6. Obtain the autocorrelation functions for Rh6G solution (*see Note 8*). The fluorescence autocorrelation functions (FAFs) from the BP505-550 nm channel, $G(\tau)$, are calculated by

$$G(\tau) = \frac{I(t)I(t+\tau)}{I(t)^2} \quad (1)$$

where τ denotes the time delay, I is the fluorescence intensity of the green channel, and $G(\tau)$ denotes the autocorrelation function of green channel.

7. The $G(\tau)$ functions are fitted with the ConfoCor 2 software installed in the LSM 510-ConfoCor 2 system. Set all parameters as free and fit the functions. After fitting the measured functions of Rh6G with a three-dimensional single-component model, determine the average structure parameter. The structure parameter, s , represents the ratio of the beam waist (w_{xy}) and the axial radius (w_z), $s = w_z / w_{xy}$. The averaged structure parameter must range from four to eight, which means that the confocal detection volume (e.g., optical setup for ConfoCor 2) is stable and best to use (*see Note 9*).

3.7 LSM and FCS Measurements for Cells

1. Observe the cells with a confocal microscope (Fig. 3a) to find a cell expressing GFP-LA at the low level, even though highly expressed cell also can be measured and analyzed (*see Note 10*).
2. Scan and image the whole cell using confocal scanning setup.
3. Select measuring positions in the nucleus of cellular image using the FCS positioning tool (Fig. 3a, cross hair).
4. For FCS measurements, set the laser intensity to 0.3 % for the 488 nm and the values of bleach time to 0 s, measuring time to 10 s, and repetition to 5. For fit condition in ConfoCor software, set the structure parameter into a value determined from Rh6G calibration measurement and set the value as fixed one.
5. Measure the selected positions and obtain autocorrelation functions for the green channel (Fig. 3b).
6. If necessary, calibrate for the real position of the FCS measurement to the position on the LSM images with a cover glass coated with dried Rh6G according to manufacturer's manual (*see Note 11*).

3.8 Curve Fitting and Data Analysis

FCS collects fluorescent signals from confocal detection volume with time for calculating fluorescence correlation function which contains parameters of molecular concentration and mobility (Fig. 4a–c). The acquired fluorescence autocorrelation functions (FAFs) are fitted using a one-component model ($i, 1$) for Rh6G in solution and a two-component model ($i, 1$ and 2) for GFP-LA in the nucleoplasm of cells, respectively, as follows:

$$G(\tau) = 1 + \frac{1 - T_{\text{triplet}} + T_{\text{triplet}} \exp^{(-\tau/\tau_{\text{triplet}})}}{(1 - T_{\text{triplet}})} \times \frac{1}{N} \sum_i y_i \left(1 + \frac{\tau}{\tau_i}\right)^{-1} \left(1 + \frac{\tau}{s^2 \tau_i}\right)^{-1/2} \quad (2)$$

Where T_{triplet} is the average fraction of triplet state molecules, τ_{triplet} is the triplet decay time (*see Note 12*), y_i is the fraction of the components, and τ_i is the diffusion time of the components. N is the average number of fluorescent molecules in the confocal volume defined by beam waist (w_{xy}) and half of the long axis (w_z) of the volume, and s is the structure parameter defined by $s = w_z / w_{xy}$. The value of s in each confocal setup is determined experimentally from the

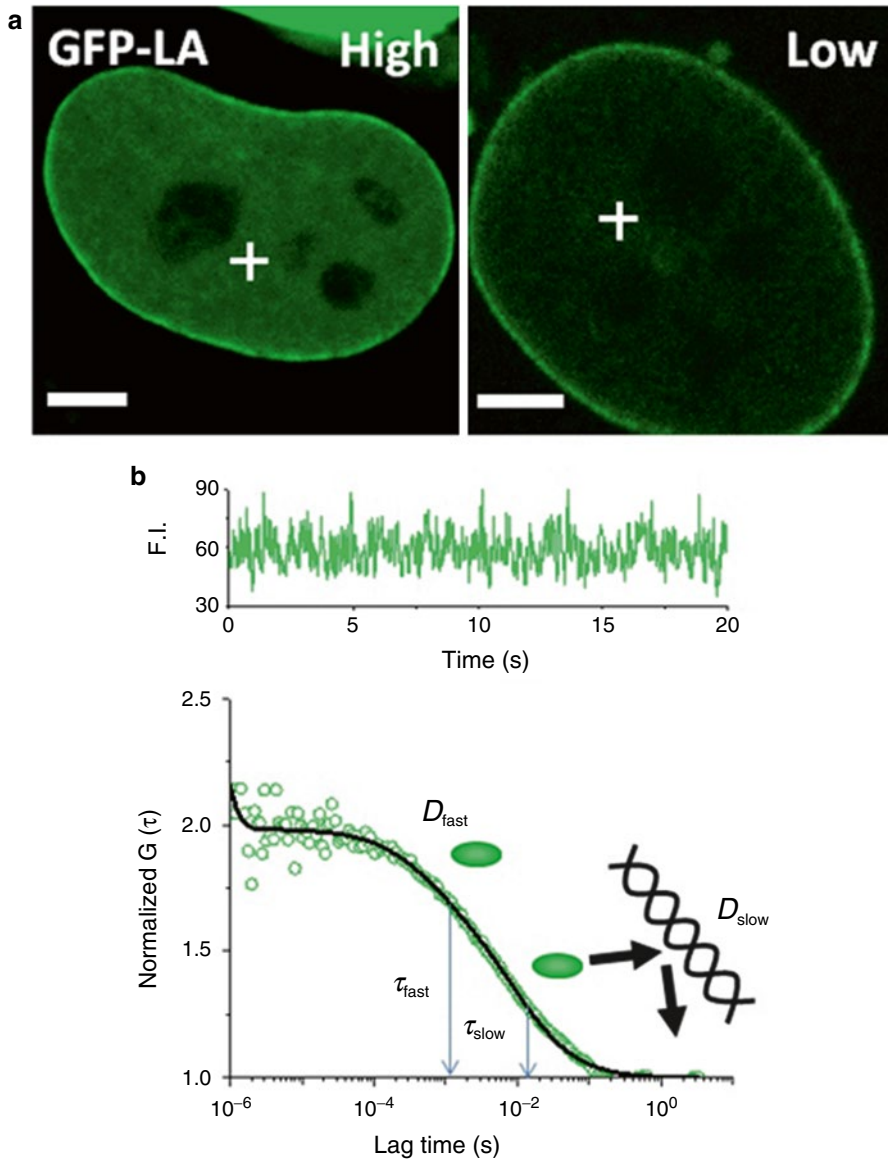


Fig. 3 Procedure of fluorescence correlation spectroscopy (FCS) measurement on GFP-LA in the nucleoplasm of living cell nuclei. **(a)** HeLa cells expressing GFP-LA at the high or low levels were selected and observed by confocal microscopy before FCS measurement. After imaging each cell, a position indicated with cross hair was measured by FCS for 10 s five times at 2-s intervals. Scale bar, 5 μm . **(b)** Averaged fluctuations of fluorescence intensity (F.I.) for GFP-LA during 20 s (*upper, green*), and the corresponding FAF (*lower, green*) were obtained from the cell expressing GFP-LA at the low level (*a, right*). Strongly expressed GFP-LA (*a, left*) was photobleached at the beginning of the measurement. A fitted function curve (*black line*) was obtained from the model equation with two-component model. It should be noted that two-component model is adapted since one-component model is not fit the measured function (see also text)

measurement of the standard dye, Rh6G. The determined value of s is fixed for fitting the autocorrelation functions obtained from cell measurements. The diffusion time (τ_i) of component i is related to the translational diffusion coefficient (D_i) of component i by

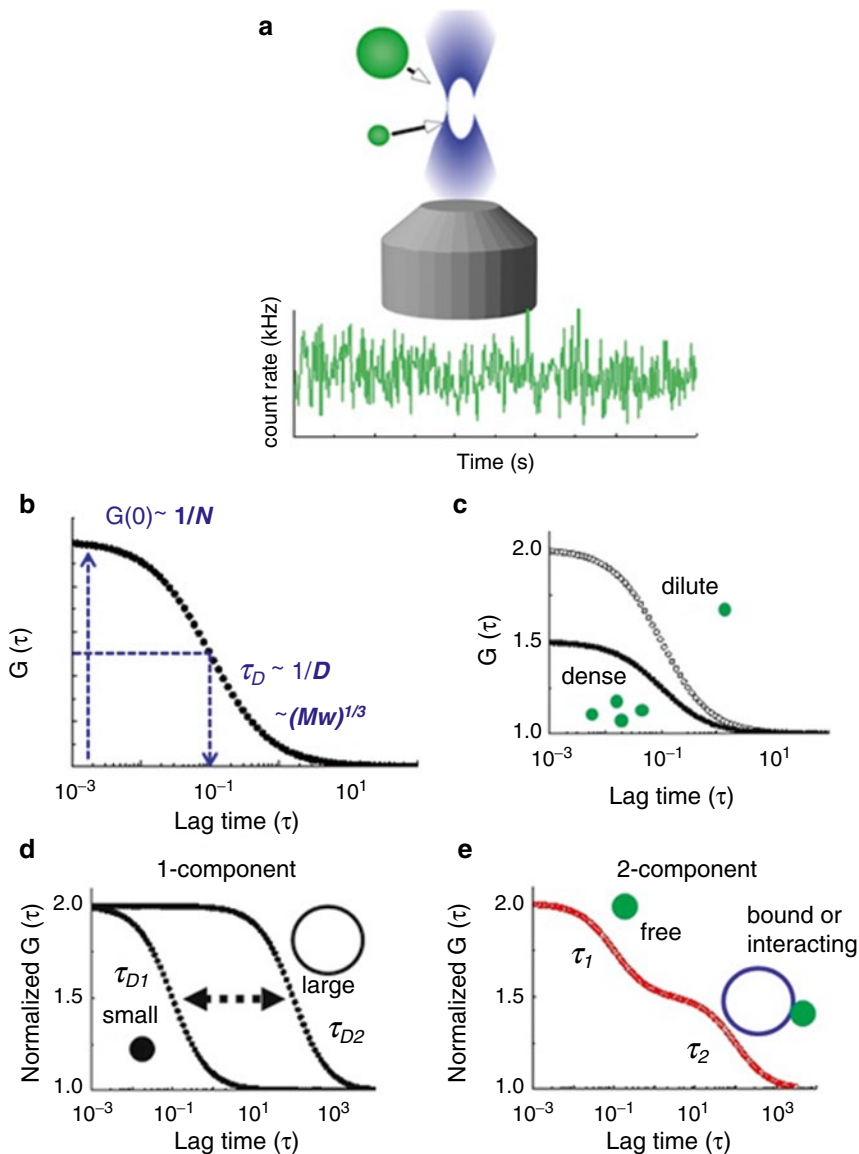


Fig. 4 Fluorescence autocorrelation functions and quantitative parameters. **(a)** FCS measurement based on fluctuation analysis of fluorescence intensity (Eq. 1). Small and large spheres tagged with fluorescent probes move in or out of the confocal volume (*white-out region in blue*) at different speeds (*top*), resulting in the characteristic fluctuation of fluorescence intensity (*bottom*). Fluorescence intensity is represented by count rate in kHz. **(b)** Measurement of single-color FCS provides a fluorescence autocorrelation function (FAF), $G(\tau)$. $G(\tau)$ allows analysis of two important physical parameters: the average number of fluorescent molecules (N) in the confocal volume and the translational diffusion time (τ_D) of the molecules through the open volume of detection (Eqs. 2 and 3). Diffusional motion of fluorescent molecules represented by τ_D or diffusion coefficient (D) reflects the molecular weight (MW) and the surrounding viscosity according to the Stokes-Einstein relation (Eq. 4). **(c)** Value of $G(0)$, correlation amplitude, is changed according to molecular number in the confocal volume as it is inversely proportional to N as shown in **(b)**. For example, two FAFs with dilute (*open circle*) and dense (*closed circle*) molecule number of the same molecular size are plotted in the graph. **(d)** Left-shifted and right-shifted FAFs plotted in the graph are obtained from FCS measurements single species of small- and

$$\tau_i = \frac{w^2}{4D_i} \quad (3)$$

The diffusion of a free (i.e., non-interacting) and spheroidal molecule is related to various physical parameters by the Stokes-Einstein equation:

$$D_i = \frac{k_B T}{6\pi\eta r_i} \quad (4)$$

where T is the absolute temperature, r_i is the hydrodynamic radius of the spheroidal molecule, η is the fluid-phase viscosity of the solvent, and k_B is the Boltzmann constant. The diffusion coefficients of GFP-LA ($D_{\text{GFP-LA}}$) in cells are calculated from the published diffusion coefficient of Rh6G, D_{Rh6G} ($280 \mu\text{m}^2/\text{s}$), the measured diffusion times of Rh6G (τ_{Rh6G}), and GFP-LA ($\tau_{\text{GFP-LA}}$) as follows:

$$\frac{D_{\text{GFP-LA}}}{D_{\text{Rh6G}}} = \frac{\tau_{\text{Rh6G}}}{\tau_{\text{GFP-LA}}} \quad (5)$$

Single-measured diffusion times and calculated diffusion coefficients obtained from one-component model analysis are represented by τ_D and D , respectively (Fig. 4b, d). If one-component model cannot fit to a measured FAF, fit the FAF with two-component model (*see Note 13*). The two mobile components of τ_1 and τ_2 (Fig. 4e) can be represented by a fast mobile (τ_{fast} or D_{fast}) and a slow mobile (τ_{slow} or D_{slow}) component (*see also Fig. 3b*).

4 Notes

1. Because it takes at least 48 h after transfection for GFP-LA to completely localize to the NL, the transfected cells should be examined at 48–72 h post-transfection by FRAP and FCS experiments.
2. GFP-LA does not properly localize to the NL when it is expressed at the very high level.
3. Start from a short-duration time for photobleaching at the maximum laser power to avoid cellular damage.

Fig. 4 (continued) large-sized molecules. Value of $G(0)$ is normalized to 2 for comparison of two different diffusions (τ_{D1} , τ_{D2}). Measured FAFs from single species of fluorescent molecules can be fitted by one-component model (*see Eq. 2*, $i=1$). (e) A FAF representing a diffusion of two species of fluorescent molecules with small to large molecular number ratio, 1:1, is plotted in the graph. Measured FAFs obtained from a solution sample or a live cell measurement with two species of fluorescent molecules can be fitted by two-component model (*see Eq. 2*, $i=2$). The one component is a fast diffusion of a freely mobile species of fluorescent molecules (*green*), and the other is a very slow diffusion of fluorescent molecules bound to large mobile or immobile targets (*blue*)

4. Because GFP-LA is immobile in the NL, time intervals and duration time for imaging can be relatively long (e.g., every 30 s for 20 min).
5. Assign one cell for FRAP experiment and another cell for showing similar GFP expression as a control.
6. Keep finding a focus including region of interest until PFS system locks on to the focus.
7. High CPM value is also dependent on precise adjustments of pinhole position and correction ring of objective corresponding to the thickness of cover glass used.
8. Other standard dyes with high fluorescence yield such as rhodamine 123 and Alexa 488 can be also used. Averaged fluorescence intensity (count per second; cps in kHz) detected by ConfoCor 2 must be temporally stationary during measurement time. If it is not, diffusion time and structure parameter deviate from ideal values when one-component model analysis is adapted. Nonstationary fluctuations of fluorescence intensity can originate from fast or slow photobleach or absorption of dye molecules into cover glass.
9. If average s value is not unstable and far from 5, repeat processes 3, 4, and 5 until the s value becomes stable.
10. The quantity of DNA plasmids used for FCS must be minimized for preparing low-expressed cells comparing to LSM measurement which images highly fluorescent cells.
11. For LSM-ConfoCor 2 system, there is a difference between measured position for FCS and selected positions on an LSM image. By tuning the real position and measuring a cell on the center of LSM image, the difference can be minimized. Newly commercialized system such as LSM780 will not need such tuning process.
12. Excitation must be optimized to minimize effect of photochemical property of GFP such as triplet and blinking.
13. Check the deviation plot obtained from one-component model curve fit, which is provided by ConfoCor 2 software. If the deviation is systematically fluctuated, it is not likely to be best fitted. In that case, use two-component model fit and then tree-component model for better fit result.

Acknowledgments

This work was supported by grants from the National Institutes of Health (GM106023) and (CA03176) Award to R.D.G.

References

1. Adam SA, Goldman RD (2012) Insights into the differences between the A- and B-type nuclear lamins. *Adv Biol Regul* 52:108–113
2. Burke B, Stewart CL (2013) The nuclear lamins: flexibility in function. *Nat Rev Mol Cell Biol* 14:13–24
3. Parry DA, Conway JF, Steinert PM (1986) Structural studies on lamin. Similarities and differences between lamin and intermediate-filament proteins. *Biochem J* 238:305–308
4. Aebi U, Cohn J, Buhle L, Gerace L (1986) The nuclear lamina is a meshwork of intermediate-type filaments. *Nature* 323:560–564
5. Schermelleh L, Carlton PM, Haase S, Shao L, Winoto L, Kner P, Burke B, Cardoso MC, Agard DA, Gustafsson MG, Leonhardt H, Sedat JW (2008) Subdiffraction multicolor imaging of the nuclear periphery with 3D structured illumination microscopy. *Science* 320:1332–1336
6. Shimi T, Pflieger K, Kojima S, Pack CG, Solovei I, Goldman AE, Adam SA, Shumaker DK, Kinjo M, Cremer T, Goldman RD (2008) The A- and B-type nuclear lamin networks: microdomains involved in chromatin organization and transcription. *Genes Dev* 22:3409–3421
7. Moir RD, Yoon M, Khuon S, Goldman RD (2000) Nuclear lamins A and B1: different pathways of assembly during nuclear envelope formation in living cells. *J Cell Biol* 151:1155–1168
8. Kochin V, Shimi T, Torvaldson E, Adam SA, Goldman A, Pack CG, Melo-Cardenas J, Imanishi SY, Goldman RD, Eriksson JE (2014) Interphase phosphorylation of lamin A. *J Cell Sci* 12:2683–2696
9. Broers JL, Machiels BM, van Eys GJ, Kuijpers HJ, Manders EM, van Driel R, Ramaekers FC (1999) Dynamics of the nuclear lamina as monitored by GFP-tagged A-type lamins. *J Cell Sci* 112:3463–3475
10. Scaffidi P, Misteli T (2005) Reversal of the cellular phenotype in the premature aging disease Hutchinson-Gilford progeria syndrome. *Nat Med* 11:440–445
11. Dahl KN, Scaffidi P, Islam MF, Yodh AG, Wilson KL, Misteli T (2006) Distinct structural and mechanical properties of the nuclear lamina in Hutchinson-Gilford progeria syndrome. *Proc Natl Acad Sci U S A* 103:10271–10276
12. Shimi T, Koujin T, Segura-Totten M, Wilson KL, Haraguchi T, Hiraoka Y (2004) Dynamic interaction between BAF and emerin revealed by FRAP, FLIP, and FRET analyses in living HeLa cells. *J Struct Biol* 147:31–41